Diffusion of Model Hydrophobic Alkali-Swellable Emulsion Associative Thickeners

Kazuomi Nagashima, Vladimir Strashko, and Peter M. Macdonald*

Department of Chemistry, University of Toronto at Mississauga, 3359 Mississauga Road, Mississauga, Ontario, Canada L5L 1C2

Richard D. Jenkins

Technical Center, Union Carbide Asia Pacific Inc, 16 Science Park Drive, #04-01/02 The Pasteur, Singapore 118227

David R. Bassett

Union Carbide Corporation, UCAR Emulsion Systems Research and Development, Cary, North Carolina 27511

Received July 25, 2000; Revised Manuscript Received October 10, 2000

ABSTRACT: Diffusion coefficients of hydrophobically modified alkali-swellable (HASE) associating polymers (APs) in aqueous solution were measured using pulsed gradient spin-echo (PGSE) nuclear magnetic resonance (NMR). HASE APs consist of a copolymer of methacrylic acid and ethyl acrylate to which hydrophobic "sticker groups" are attached through a poly(ethylene oxide) (PEO) "spacer arm". Two series of HASE APs were investigated: one in which the length of the hydrophobic alkyl chain was varied (C_xE_{35}) and another in which the length of the PEO spacer arm was varied ($C_{20}E_y$). With increasing hydrophobe or PEO spacer arm length the average diffusion coefficient decreased, reflecting the viscosity enhancement produced by the associating network formed by HASE polymers. The effect of external variables such as concentration, pH, and temperature mirrored established rheological properties for such systems. The average diffusion behavior, however, was the result of a superposition of two contributions, one slow ($D_0 < 1 \times 10^{-11}$ m^2 s^{-1}) and one fast ($D_0 \approx 1 \times 10^{-10}$ m^2 s^{-1}) diffusing. Changing the hydrophobe chain length or the PEO spacer arm length modulated the proportion of the fast and slow diffusing populations but had relatively little effect on the diffusion coefficients of the two populations. Precipitation of the HASE AP from THF−HCl_{aq} produced two fractions, one enriched with hydrophobe and the other correspondingly depleted relative to the global average. The fractions enriched and depleted with respect to hydrophobe exhibited diffusion coefficients similar to the fast and slow diffusing populations. We conclude that the hydrophobe is inhomogeneously distributed among the HASE AP chains, that the population enriched with hydrophobe forms more compact structures capable of faster diffusion, and that the effects of hydrophobe chain length and PEO spacer arm length on HASE AP solution viscosity are mediated by their influence on the coupling of the hydrophobe enriched population into the slow-diffusing hydrophobe-depleted population.

Introduction

Water-borne systems are fast replacing traditional solvent-based formulations in many commercial applications, in response to the need to eliminate the release of volatile organic components (VOC) into the environment. In the search to maintain performance and to achieve the desired rheological properties in water-borne systems, attention has turned to hydrophobically modified water-soluble polymers.[1] Their hydrophobic "sticker" groups form transient associations with one another and with other formulation constituents, such as surfactant, latex, and pigment. The resulting transient network displays desirable rheological behavior such as high viscosity at low shear combined with low viscosity at high shear.

A number of different hydrophobically modified water-soluble polymers have been investigated with a view to describing their modes of association and the origin of their complex rheological behavior. The most thoroughly investigated are the end-capped or telechelic associating polymers (APs), such as the HEUR (hydrophobically modified ethoxylated urethane) APs based on poly(ethylene oxide).[2−6] End-capped APs self-associate into discrete micelles or "rosettes" consisting of a core of hydrophobic groups surrounded by a corona of polymer chains looping back into the core. Increasing polymer concentration produces an increase in the number of "linking" chains bridging between rosettes, leading to network propagation.

Comb APs contain multiple pendant hydrophobic stickers distributed along the length of the water-soluble polymer backbone. In principle, there are many such structures, when one considers the variables of hydrophobe structure, numbers of hydrophobes, their distribution along the chain, and the structure of the polymer chain itself. For example, there is a substantial literature describing acrylate and acrylamide copolymers,[1a−d] wherein the hydrophobes tend to be bunched rather than randomly distributed along the polymer backbone. Comb APs based on poly(ethylene oxide) have been synthesized with a random distribution of hydrophobes.[7] These likewise associate into micelle-like structural units and form networks at higher concentrations, with shear thinning occurring only above a critical shear rate.

* To whom correspondence should be addressed. Tel 905 828 3805; fax 905 828 5425; e-mail pmacdona@credit.erin.utoronto.ca.

10.1021/ma0013004 CCC: $19.00
Published on Web 11/22/2000

Hydrophobically modified hydroxyethylcellulose (HMHEC) is another class of technologically important AP.[8−14] Here, hydrogel formation is observed, and the stiffness of the cellulosic water-soluble backbone limits the number of hydrophobes in an association cluster, relative to the number observed with flexible poly(ethylene oxide)-based APs.

Recently, a new class of AP has emerged, in which the comblike hydrophobic stickers are separated from the polymer backbone, typically a copolymer of methacrylic acid and ethyl acrylate, by the presence of a poly(ethylene oxide) (PEO) "spacer" arm.[15,16] These hydrophobically modified alkali-swellable emulsion (HASE) polymers are insoluble at low pH. Alkaline pH ionizes the acid groups, leading to swelling of the resulting polyelectrolyte and solubility in water. Thus, thickening by HASE polymers occurs by both an associative mechanism and an expansion of the polymer backbone. With increasing HASE AP concentration, a transformation takes place from predominantly intramolecular hydrophobic associations to predominantly intermolecular hydrophobic associations, leading to network formation. Rheological studies on model HASE APs reveal viscosity enhancement at low shear followed by shear thinning above a critical shear rate.[16] The details are dependent on the lengths of the PEO spacer arm and hydrophobe. In addition, such studies showed that surfactants have striking effects on network junction numbers and lifetimes, enhancing network strength below a critical surfactant concentration, while disrupting the network at higher concentrations. The viscoelastic properties of the network are characterized by two distinct relaxation times,[16c] as opposed to the single relaxation time characterizing network dynamics in HEUR AP systems.[4]

An understanding at the molecular level of the mechanism of rheological modification by APs has evolved only by assembling results from a multitude of techniques. The HEUR APs, arguably the best understood of the APs, have been studied intensively by a combination of molecular level techniques (fluorescence and nuclear magnetic resonance spectroscopies) with mesoscopic (dynamic and static light scattering) and macroscopic (rheology) measurements, supported by theoretical modeling of network formation.

For the HASE APs, there is a growing rheology literature[16] examining the effects of structural variables, such as the lengths of the hydrophobe[16c] and the PEO spacer arm,[16d] and formulation variables, such as temperature,[16e] ionic strength,[16f] and surfactant addition.[16g] These have been augmented by fluorescence studies of the nature of the hydrophobic domains formed by HASE APs,[17] intrinsic viscosity measurements as a function of ionic strength and hydrophobe length,[18] isothermal titration calorimetry studies of surfactant interactions,[19] and static and dynamic light scattering studies of HASE AP microstructure.[20]

Nevertheless, the microstructure of HASE AP networks is still poorly understood. Here we describe pulsed gradient spin-echo (PGSE) nuclear magnetic resonance (NMR) measurements of polymer diffusion in solutions of model HASE polymers having different lengths of the PEO spacer arm and the hydrophobic sticker group. Diffusion measurements provide a molecular level perspective on network strength and ramification through the solution. Our immediate goal here is to correlate HASE AP diffusion coefficients with rheological, spectroscopic, and other measurements performed previously.[16−20] The long-term goal is to achieve a molecular level understanding of the association mechanism of these structurally and rheologically complex polymers.

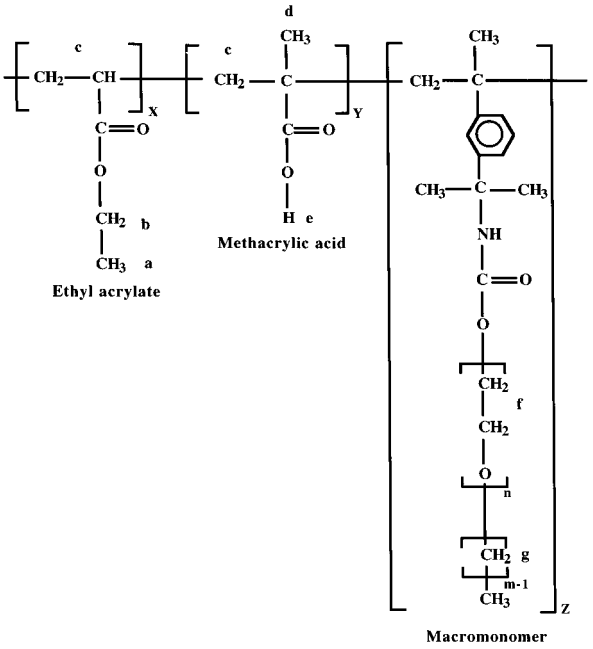

Figure 1. Structure of the HASE APs, consisting of a random copolymer of ethyl acrylate (molar ratio *X*), methacrylic acid (molar ratio *Y*), and a hydrophobically modified macromonomer (molar ratio *Z*). Values of *X*, *Y*, and *Z* are determined from ^{1}H NMR spectroscopy as described in the text and detailed in Table 2. The chemical groups labeled with lower case letters are assigned to the ^{1}H NMR resonances shown in Figure 2 having the frequencies listed in Table 1.

Experimental Section

Sample Preparation. The general structure of the HASE APs is shown in Figure 1. They consist of a backbone of methacrylic acid (MA) and ethyl acrylate (EA) copolymerized with a number of associative macromonomers (MM). The latter contains a linear alkyl chain hydrophobe (designated C_x where *x* is the number of carbons in the alkyl chain) joined to the polymer backbone through a dimethyl *m*-isopropenylbenzyl isocyanate/PEO bridge (designated E_y where *y* is the number of ethylene oxide units). Two series of HASE APs were investigated here: one in which the hydrophobe chain length is held constant while the PEO spacer arm of the macromonomer is varied in length ($C_{20}E_0$, $C_{20}E_{10}$, $C_{20}E_{15}$, $C_{20}E_{35}$, and $C_{20}E_{40}$) and a second in which the PEO spacer arm length is held constant while the chain length of the hydrophobe is varied (C_4E_{35}, C_8E_{35}, $C_{12}E_{35}$, $C_{16}E_{35}$, and $C_{20}E_{35}$). The synthesis and characterization of the HASE APs have been described in detail.[15b] Their viscosity-average molecular weights are of the order of 200 000.

Prior to preparation of aqueous solutions, the polymers were recrystallized from ethyl acetate followed by extended dialysis in cellulose membranes with frequent changes of water and finally lyophilization. A stock solution of 2 wt % polymer in 99.9% deuterium oxide, pD = 9.3, was prepared by hydrating lyophilized polymer for a period of 24 h. The final pD was corrected to 9.25 using 1.0 M KOD in deuterium oxide. All other polymer concentrations were prepared by serial dilution into NMR tubes. These were then sealed and stored in the dark at 4 °C until use.

NMR Spectroscopy. Proton NMR spectra of the HASE APs, their constituent monomers, and, where possible, the corresponding homopolymers were obtained using a Varian UNITY 400 NMR spectrometer operating at 399.4 MHz for protons and equipped with a high-resolution quadnuclei probe

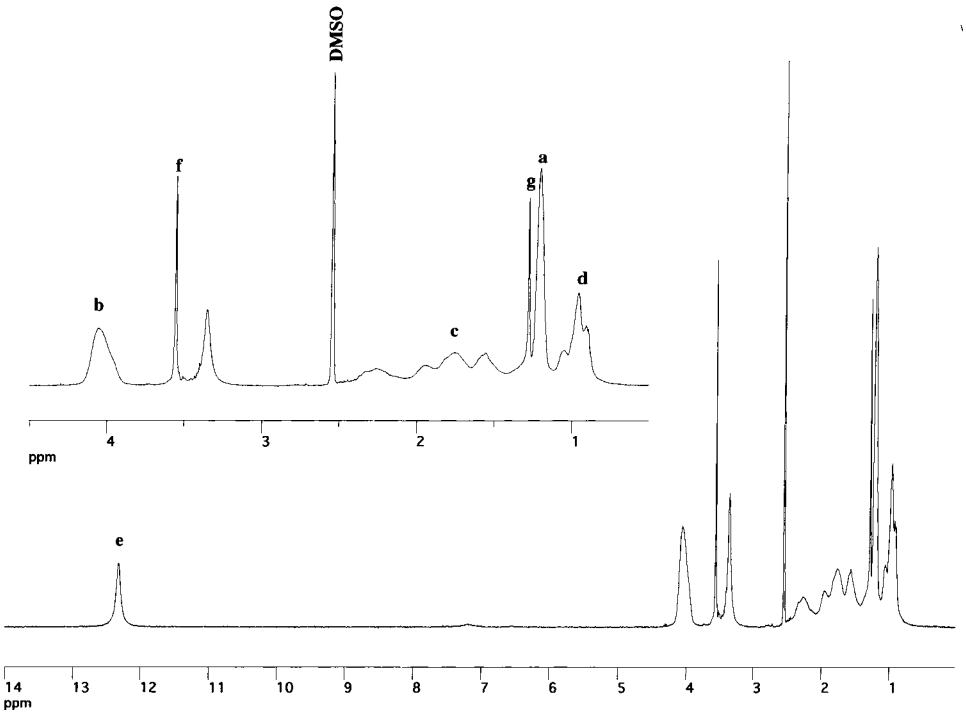

Figure 2. The 400 MHz ^{1}H NMR spectrum of HASE AP $C_{20}E_{35}$ in DMSO-d_6. The resonances labeled with lower case letters are assigned to particular chemical groups in the polymer as shown in Figure 1, with frequencies listed in Table 1. The resonances of the poly(ethylene oxide) (PEO) and the hydrophobic group (R) of the macromonomer were particularly simple to assign by virtue of their intensity variations across the two HASE AP series $C_{20}E_y$ and C_xE_{35}. The exchangeable proton of the methacrylic acid was assigned to the resonance "e" which vanishes in D_2O. In general, it is not possible to assign all of the polymer backbone resonances due to their breadth and the complexity of copolymer statistics. The polymer compositions calculated from such spectra are listed in Table 2.

Table 1. ^{1}H NMR Resonance Assignments for HASE APs

reson[a]	chem shift (ppm)	assignment [b]
a	1.2	EA ethyl ester methyl
b	4.05	EA ethyl ester methylene
c	1.4−2.0	EA and MA backbone methylenes
d	0.97	MA methyl
e	12.35	MA carboxyl
f	3.58	MM ethylene oxide
g	1.28	MM hydrophobe

[a] Letter assignments given in Figure 1 correspond to resonances in Figure 2. [b] Assignments were made on the basis of comparisons with spectra of corresponding monomers and homopolymers and by comparing across the two series $C_{20}E_y$ and C_xE_{35}.

(Nalorac, Martinez, CA). Typically, 32 transients were signal averaged, each consisting of 8192 data points covering a spectral width of ±3750 Hz, recorded following a single 90° pulse (6.3 μs) excitation with a 1.1 acquisition time and a 20 s relaxation delay. The free induction decays were Fourier transformed after exponential line broadening (1 Hz) and zero filling to 16 384 data points. Figure 2 shows a typical ^{1}H NMR spectrum of a HASE AP dissolved in DMSO-d_6 (Cambridge Isotopes, Andover, MA) at a concentration of 2% w/v. The chemical shifts were referenced to the residual DMSO proton resonance at 2.54 ppm. The resonance assignments, corresponding to the lettering scheme in Figure 1, are listed in Table 1. The assignments were made on the basis of comparisons of 1D ^{1}H NMR and 2D ^{1}H−^{1}H COSY NMR spectra of corresponding monomers and, where possible, homopolymers and by comparing across the series of HASE APs.

Proton NMR self-diffusion measurements were performed using an MRI (magnetic resonance imaging) probe with actively shielded gradient coils (Doty Scientific, Columbia, SC) installed in a Chemagnetics CMX300 NMR spectrometer operating at 299.5 MHz for protons. Diffusion coefficients were determined using the PGSE (pulsed gradient spin-echo) technique[21a] with the following typical parameters as indicated in parentheses: 90° pulse length (22.5 μs), interpulse delay (τ = 50 ms), and recycle delay (5 s). The gradient pulse was applied along the *z*-direction for durations varying between 2 and 32 ms. Two different gradient amplitudes were employed: a lower amplitude of ∼35 G cm^{-1} for water diffusion and a higher amplitude of ∼200 G cm^{-1} for polymer diffusion. The lower gradient amplitude was calibrated using the known diffusion coefficient of 2 vol % water in deuterium oxide (D_0 = 1.9 × 10^9 m^2 s^{-1})[22] while the higher gradient amplitude was calibrated using a 9.5 wt % PEO (M_w = 6000) in water solution in which the diffusion coefficient could be measured at either gradient strength. No echo distortion or drift due to eddy currents was observed under these conditions. Typical signal acquisition conditions were a spectral width of 10 kHz, digitized into 512 data points, with a 0.512 s acquisition time and a 5 s relaxation delay. Although the number of transients varied depending on the length of the PEO spacer arm, typically at least 512 transients were signal averaged for any one value of the gradient pulse length. The data were processed with an exponential line broadening corresponding to 10 Hz and zero filled to 2048 points prior to Fourier transformation. The sample temperature was controlled to 25 °C unless otherwise indicated.

From the attenuation of the NMR resonance intensities as a function of the gradient pulse length, one may measure the self-diffusion coefficient of the polymer according to eq 1,

$$I/I_0 = \exp[-(\gamma G\delta)^2(\Delta - \delta/3)D] \quad (1)$$

which relates the resonance intensity "I" observed for a particular duration "δ" of the gradient pulse in the PGSE NMR experiment to the intensity in the absence of any field gradient pulse "I_0", where γ is the magnetogyric ratio of the observed nucleus, G is the calibrated gradient strength, Δ is the separation between the pair of gradient pulses in the PGSE pulse sequence, and D is the corresponding diffusion coefficient.[21a] The diffusion coefficient is measured from the slope in a plot of the logarithm of the signal intensity versus $\delta^2(\Delta - \delta/3)$,

assuming the value of the gradient strength is known from a calibration experiment as described above.

Results and Discussion

Composition of the HASE APs via ^{1}H NMR. A first priority was to determine the monomer composition of the HASE APs from high field proton NMR measurements. For these measurements, the HASE APS were desiccated from 5 wt % aqueous polymer solutions adjusted to pH 3 and then dissolved in DMSO-d_6. The purpose here was to protonate all carboxyl groups. The resulting ^{1}H NMR spectrum is shown in Figure 2, with resonances assigned according to the lettering scheme shown in Figure 1, as detailed in Table 1. In general, it is not possible to assign entirely the EA and MA backbone resonances, given their breadth and the complexities of polymer statistics for random copolymers such as these. Nevertheless, certain readily resolved resonances permit characterization of the HASE AP chemical composition. Specifically, the ethyl ester methylene protons of EA at 4.05 ppm (b) and the acidic proton of the MA carboxyl group at 12.35 ppm (e) are readily resolved and free from overlap with other resonances. The ethylene oxide protons of the PEO spacer arm of the MM occur at 3.58 ppm (f) and, likewise, are resolved readily.

Table 2 shows the molar composition of the various HASE APs utilized here, as determined by comparing the integrated intensities of their characteristic ^{1}H NMR resonances. Generally, their compositions lie close to the EA/MA/MM molar ratios of 49.5:49.5:1.0 expected from the synthetic conditions.[15] Significant deviations do occur, however, notably with respect to the MM content, which often fell well below 1 mol %. We note that in calculating the MM content we have assumed that the length of the PEO spacer arm is uniform and precise.[15] We note further that the compositional information represents a global average and provides no details regarding compositional heterogeneity within the population of polymer chains.

Dissolution of HASE APs. As synthesized, HASE APs form latex particles. Studies of the dissolution behavior of HASE APs in water have demonstrated that increasing the degree of ionization of the polymer's MA units encourages the initial latex particle to swell and eventually dissolve.[16b] The dissolution process proceeds due to the charge repulsion within and between individual polymer chains and involves water penetration into the latex followed by chain disentanglement.

The high-resolution ^{1}H NMR spectrum of the HASE APs in the form of latex particles, i.e., prior to dissolution by increasing pH, shows no visible resonances assignable to the polymer. Such solutions are turbid but not particularly viscous. Failure to observe ^{1}H NMR resonances from the HASE APs can be attributed, therefore, to dipolar line broadening arising from slow rotational tumbling of the latex particles (hydrodynamic radius of 75 nm) combined with immobilization of individual polymer molecular segments due to the low water content within the latex particles (roughly 30 wt %).[16c]

With increasing pH and degree of neutralization of the HASE AP's MA groups, resonances attributable to the polymer begin to appear in the high-resolution ^{1}H NMR spectrum. Complete neutralization requires a pH greater than 9.0.[16c] At such a pH, aqueous solutions of HASE AP are clear and highly viscous, since dissolution of individual polymer chains is complete and hydrophobic associations lead to network formation.

Table 2. Composition of HASE APs from ^{1}H NMR

resonance[a]	no. of protons (nominal)	intensity absolute[b]	intensity normalized[c]	comp (mol %)
		$C_{20}E_0$		
MA	1	1000	1000	53.8
EA	2	1719	860	46.2
MM	0	0	0	0
		$C_{20}E_{10}$		
MA	1	1000	1000	40
EA	2	2930	1465	58.7
MM	40	1304	33	1.3
		$C_{20}E_{15}$		
MA	1	1000	1000	50.1
EA	2	1967	983	49.2
MM	60	822	14	0.7
		$C_{20}E_{35}$		
MA	1	1000	1000	47.8
EA	2	2151	1075	51.4
MM	140	2488	18	0.8
		$C_{20}E_{40}$		
MA	1	1000	1000	49.9
EA	2	1988	994	49.6
MM	160	1833	11	0.5
		C_4E_{35}		
MA	1	1000	1000	53.3
EA	2	1715	858	45.7
MM	140	2456	17.5	1
		C_8E_{35}		
MA	1	1000	1000	50.8
EA	2	1900	950	48.2
MM	140	2800	20	1
		$C_{12}E_{35}$		
MA	1	1000	1000	41.3
EA	2	2818	1409	58.2
MM	140	1888	13.5	0.5
		$C_{16}E_{35}$		
MA	1	1000	1000	50.5
EA	2	1925	962	48.6
MM	140	2554	18.2	0.9

[a] MA refers to resonance "e" assigned to the MA carboxyl proton, EA refers to resonance "b" assigned to the EA ethyl ester methylene protons, while MM refers to resonance "f" assigned to the MM ethylene oxide protons. [b] Intensity of MA resonance is normalized to 1000 in each case. [c] Intensities are normalized with respect to the nominal number of protons giving rise to that resonance.

The corresponding ^{1}H NMR spectra contain two readily resolvable resonances in addition to the water resonance: one corresponding to the EO protons of the PEO spacer arm and the other originating from unresolved contributions from polymeric backbone methyl and hydrophobe methylene protons. Their line widths indicate relatively high local mobility of the polymer molecular segments, despite the entrapment of entire polymer chains in an extended associating network. The line widths are still broad, however, relative to those observed for the same HASE APs dissolved in DMSO where network formation is expected to be minimal. We note, as well, that further line narrowing is obtained in these situations when the HASE AP samples are spun rapidly in a magic angle spinning (MAS) NMR probe. This indicates that residual dipolar interactions contribute to the observed line broadening in aqueous solutions of HASE APs. It is not possible, however, to perform PGSE NMR diffusion measurement on rapidly spinning samples.

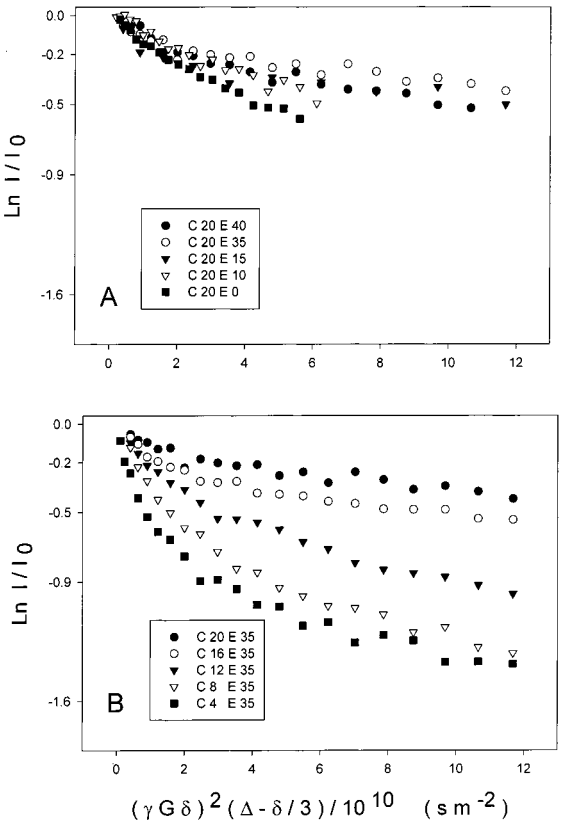

Figure 3. HASE AP PEO resonance intensity attenuation in the PGSE NMR experiment as a function of (panel A) PEO chain length in the series $C_{20}E_x$ and (panel B) hydrophobe chain length in the series C_xE_{35}. All data shown are for 2 wt % HASE AP in D_2O, pD = 6.5, and $G = 235$ G cm^{-1}.

These preliminary measurements indicate that ^{1}H NMR diffusion studies on HASE AP solutions can be carried out readily only after dissolution of the original latex particles has occurred. The water resonance does not interfere with the analysis since diffusion of water is rapid, producing rapid attenuation of its resonance intensity at the gradient strengths employed to observe polymer diffusion. Since the PEO resonances are, by far, the most intense in spectra of HASE APs, their intensity was used to obtain diffusion coefficients.

Qualitative Analysis of HASE AP Diffusion. Figure 3 illustrates the attenuation of the spectral intensity of the PEO protons with increasing gradient pulse duration for the different HASE APs investigated here, all at 2 wt % concentration. Figure 3A shows the $C_{20}E_x$ series, having different lengths of the PEO spacer arm, while Figure 3B shows the C_xE_{35} series, having different lengths of the hydrophobic sticker group.

In general, greater attenuation for a given value of $\delta^2(\Delta - \delta/3)$ equates to faster diffusion. Superficially, therefore, one concludes that for the $C_{20}E_y$ series the slowest diffusion is observed for the $C_{20}E_{35}$ HASE AP and that, in general, a shorter PEO spacer arm yields a faster diffusing species. Rheological studies of low shear viscosity in HASE AP solutions versus PEO spacer arm length indicate that optimal viscosity enhancement is obtained with a PEO spacer arm having 35 EO units.[16h] Qualitatively, therefore, the PGSE NMR and rheology studies concur. The PGSE NMR results in Figure 3B indicate that HASE AP diffusion slows progressively as the length of the hydrophobe increases. This agrees with rheology data indicating that low shear viscosity increases with increasing number of carbons in the HASE AP hydrophobe.[16c] Therefore, since higher viscosity equates to slower diffusion, the rheology and PGSE NMR findings agree with respect to the effects of PEO and hydrophobe chain length on HASE AP network formation.

However, for the case of a single characteristic diffusion coefficient the intensity decay should be exponential, and a plot of the logarithm of the signal intensity versus $(\gamma G\delta)^2(\Delta - \delta/3)$, as per eq 1 and as shown in Figure 3, should be linear with a slope proportional to the diffusion coefficient. The signal intensity decays in Figure 3 are clearly nonlinear. This is particularly obvious for the C_xE_{35} series in Figure 3B. Any analysis of the diffusion properties of the various HASE APs must first address the origin of this behavior.

PGSE NMR signal attenuation of the type shown in Figure 3 has several possible origins, one being the presence of restricted diffusion. This arises when the diffusing entity encounters barriers to diffusion which are separated by distances short relative to the diffusion distance characteristic of the particular experiment. The latter depends on the diffusion coefficient and the experimental diffusion time according to the Einstein relationship,

$$\langle x^2\rangle^{1/2} = 2Dt \qquad (2)$$

where $\langle x^2\rangle^{1/2}$ is the root-mean-square diffusion distance and $t = \Delta - \delta/3$ is the diffusion time for the PGSE NMR experiment. If restricted diffusion is present, the signal attenuation in the PGSE NMR experiment will be nonexponential at longer diffusion times (larger values of Δ) but will approach exponential behavior with shorter diffusion times (smaller values of Δ).[21b]

Figure 4A shows intensity attenuation curves obtained with a 2 wt % solution of $C_{20}E_{40}$ at four different experimental diffusion times, corresponding to values of Δ ranging from 50 to 125 ms. The signal intensity attenuations overlap for all values of Δ. Therefore, if restricted diffusion is present, the barrier separation is so narrow relative to the rms diffusion distance that reducing the experimental diffusion time by a factor of more than 2 has little effect. As we demonstrate later, similar nonexponential decays are observed even at low HASE AP concentrations, where restriction barriers should be more widely separated. We conclude that restricted diffusion is not the most likely explanation for the observed signal attenuation behavior.

A second possible source of nonexponential decay in the PGSE NMR experiment is the presence of a continuous (monomodal) distribution of diffusion coefficients about some average. Any situation in which there is a distribution of sizes of the diffusing units produces such an effect. This includes polydispersity of polymer molecular weight[23] and polydispersity of cluster size in coupled clusters of associating polymers.[24] For systems with a continuous size distribution, a stretched exponential has been found to adequately represent the data, as per eq 3,

$$I = I_0 \exp\{-[(\gamma G\delta)^2(\Delta - \delta/3)D_e]^\beta\} \qquad (3)$$

where the parameter β is a measure of the width of the distribution of diffusion coefficients, and $0 \le \beta \le 1$, so that for a monodisperse diffusion coefficient $\beta = 1$ and eq 3 reverts to eq 1.[25]

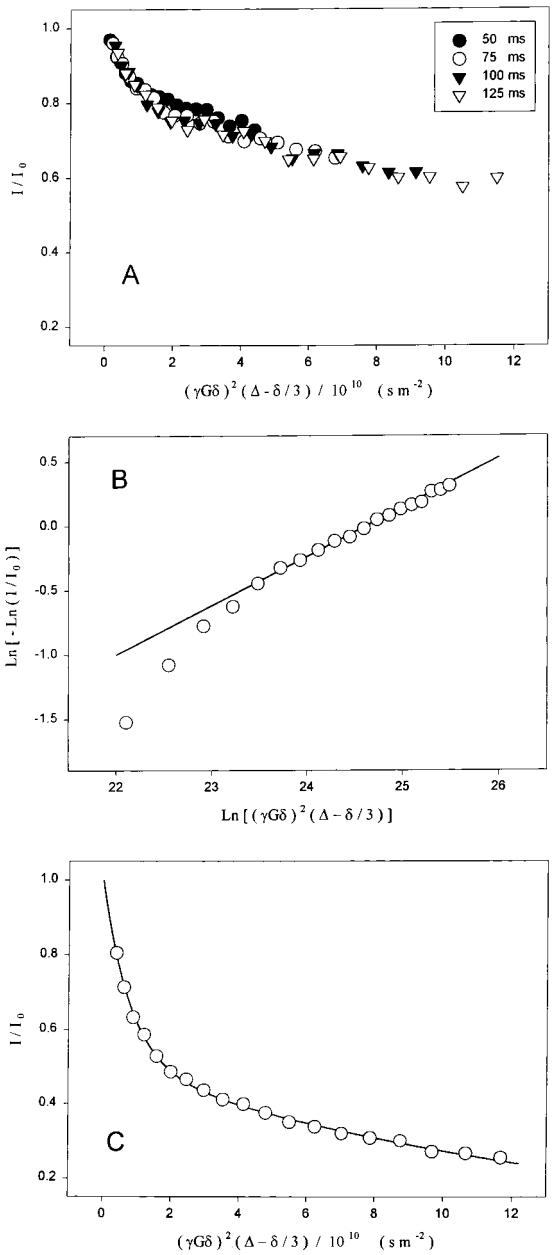

Figure 4. (A) HASE AP PEO resonance intensity attenuation in the PGSE NMR experiment as a function of the diffusion time Δ for the case of 2 wt % $C_{20}E_{40}$ in D_2O at pD = 6.5. Since all curves for different diffusion times are superimposed, restricted diffusion is eliminated as an explanation for the nonexponential decay of the signal intensity. (B) HASE AP PEO resonance intensity attenuation in the PGSE NMR experiment as per a linearized form of eq 3 for the case of 2 wt % $C_{20}E_{35}$ in D_2O, pD = 6.5, and G = 235 G cm^{-1}. A continuous distribution of diffusion coefficients about a single mean value would yield a straight line with slope equal to β and intercept equal to β ln D, where β is defined in the text. The data clearly indicate at least a bimodal distribution of diffusion coefficients. (C) HASE AP PEO resonance intensity attenuation in the PGSE NMR experiment fit assuming a bimodal distribution of diffusion coefficients, as per eq 4, for the case of 2 wt % $C_{20}E_{35}$ in D_2O, pD = 6.5, and G = 235 G cm^{-1}. In this instance $X_s = 0.836$, $D_s = 1.9 \times 10^{-12}$ m^2 s^{-1}, $X_f = 0.164$, and $D_f = 8.2 \times 10^{-11}$ m^2 s^{-1}.

Figure 4B shows the fit of the signal attenuation data to a linearized version of eq 3.[26] For the case of a continuous distribution, $\ln[-\ln(I/I_0)]$ should vary in a linear fashion with $\ln[(\gamma G\delta)^2(\Delta - \delta/3)]$. This is not observed for the case shown in Figure 4B or any of the other HASE APs examined in this study. We conclude that the distribution of diffusion coefficients is not monomodal continuous.

A third possible source of nonexponential decays in the PGSE NMR experiment is the presence of a discontinuous or discrete distribution of diffusion coefficients (bimodal or greater). For the case of two populations in slow exchange with one another on the NMR time scale, the intensity will attenuate in the PGSE NMR experiment according to eq 4,

$$I/I_0 = X_s \exp(-kD_s) + X_f \exp(-kD_f) \qquad (4)$$

where $k = [(\gamma G\delta)^2(\Delta - \delta/3)]$, X_i and D_i are the mole fractions and diffusion coefficients of the two components, and the subscripts "s" and "f" refer to the slower and the faster diffusing components, respectively. As shown in Figure 4C, a satisfactory fit to the signal intensity attenuation data for the HASE APs is obtained by assuming such a bimodal distribution of diffusion coefficients. (For the case of fast exchange, the observed intensity attenuates as a single exponential, weighted according to the diffusion coefficients and populations of the contributing species.)

It is possible that the distribution of diffusion coefficients in the HASE AP solutions is more than bimodal. However, assuming a more complex distribution does not improve the quality of fits to the data. A more rigorous divination of the nature of the distribution could involve 2D pulsed field gradient experiments such as the diffusion-ordered 2D NMR technique of Morris and Johnson[27] but lies beyond the scope of this study. For the present, it appears satisfactory to conclude that there is a bimodal distribution of diffusion coefficients in the HASE AP solutions, corresponding to faster and slower diffusing species in slow exchange with one another. In support of this contention, we note that a recent light scattering study of HASE AP $C_{16}E_{35}$ likewise concluded that solutions of such polymers display two populations, differing with respect to their diffusion coefficients.[20] One population was considered to consist of large aggregates containing up to five polymer chains, while the other consisted of individual polymer chains having multiple intramolecular associations.

Quantitative Analysis of HASE AP Diffusion. Figure 5 illustrates how the diffusion coefficient of the fast and slow diffusing populations vary in the HASE APs as a function of the two structural variables of PEO spacer arm length and hydrophobe chain length, according to eq 4.

The diffusion coefficients of the fast and slow diffusing populations differ by at least an order of magnitude. With increasing PEO spacer arm length D_s decreases and D_f increases systematically (Figure 5A). With increasing hydrophobe chain length the diffusion coefficient of the slow diffusing species D_s decreases progressively, while that of the fast diffusing species D_f is relatively unaffected (Figure 5B). In absolute terms, the values of the diffusion coefficients of the two populations as shown in Figure 5 are comparable in magnitude to those of the two populations observed via light scattering studies of HASE AP $C_{16}E_{35}$.[20]

Figure 6 illustrates the manner in which the fraction of the fast and slow diffusing populations varies in the HASE APs as a function of the two structural variables of PEO spacer arm length and hydrophobe chain length, as per eq 4.

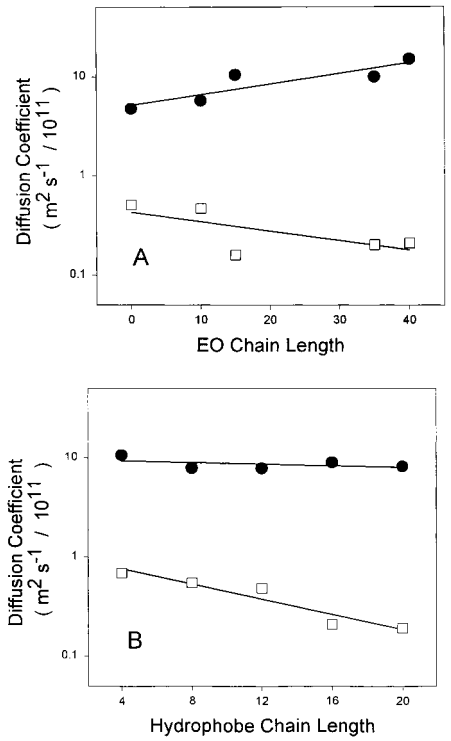

Figure 5. (A) Diffusion coefficients of the slow (D_s, open squares) and the fast (D_f, closed circles) diffusing components as a function of the PEO chain length. All HASE APs were present at 2 wt % in D_2O, pD = 6.5, and G = 235 G cm^{-1}. Diffusion coefficients were obtained by fitting eq 4 to HASE AP PEO resonance intensity attenuation data. (B) Diffusion coefficients of the slow (D_s, open squares) and the fast (D_f, closed circles) diffusing components as a function of the hydrophobe chain length. All HASE APs were present at 2 wt % in D_2O, pD = 6.5, and G = 235 G cm^{-1}. Diffusion coefficients were obtained by fitting eq 4 to HASE AP PEO resonance intensity attenuation data.

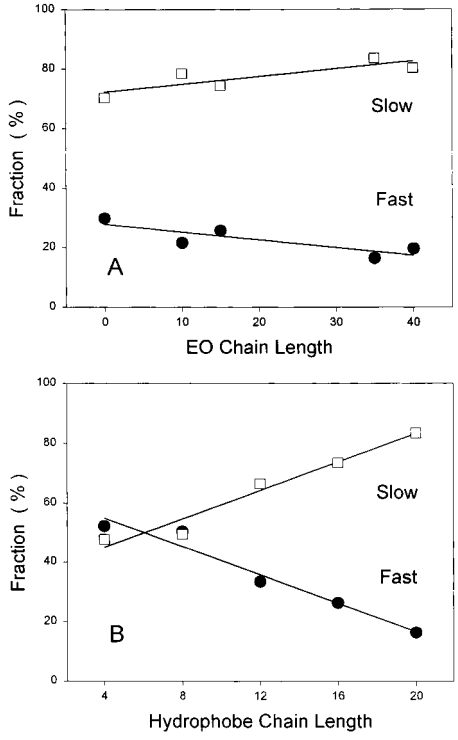

Figure 6. (A) Fractional compositions of the slow (X_s, open squares) and the fast (X_f, closed circles) diffusing components as a function of the PEO chain length. All HASE APs were present at 2 wt % in D_2O, pD = 6.5, and G = 235 G cm^{-1}. Mole fractions were obtained by fitting eq 4 to HASE AP PEO resonance intensity attenuation data. (B) Fractional compositions of the slow (X_s, open squares) and fast (X_f, closed circles) diffusing components as a function of the hydrophobe chain length. All HASE APs were present at 2 wt % in D_2O, pD = 6.5, and G = 235 G cm^{-1}. Mole fractions were obtained by fitting eq 4 to HASE AP PEO resonance intensity attenuation data.

In Figure 6A, one sees that the fraction of fast diffusing species X_f decreases, from about 30% to about 20%, with a corresponding increase in the fraction of slow diffusing species, as the length of the PEO spacer increases. In Figure 6B, it is evident that with increasing hydrophobe chain length the HASE AP solution changes progressively from an approximately equal mixture of slow and fast diffusing populations for the case of C4 hydrophobes to one consisting almost entirely of the slow diffusing population for the case of C20 hydrophobes.

For the specific case of the $C_{16}E_{35}$ HASE AP investigated by light scattering,[20] at concentrations below roughly 0.1 wt %, it was found that 35 wt % of the polymer chains were distributed in the fast diffusing, essentially unimeric population, while the remaining 65 wt % were distributed in a slow diffusing population consisting of aggregates containing approximately five unimers. The distribution between the fast and slow diffusing populations observed via PGSE NMR for the HASE AP $C_{16}E_{35}$ agrees with the light scattering results. It should be borne in mind that, as employed here, PGSE NMR detects the distribution of PEO spacer arms between the fast and slow diffusing populations, since this is the largest resonance in the NMR spectrum and was that used to measure diffusive signal attenuation. Only if the macromonomer distribution is homogeneous across all polymer chains will the behavior of the PEO spacer arm faithfully reflect that of the polymer chains themselves.

Table 3. Concentration, pH, and Temperature Effects on C_8E_{35} HASE AP Diffusion

	$D_f/10^{-10}$ m^2 s^{-1}	$D_s/10^{-11}$ m^2 s^{-1}	X_f	X_s
concn (wt %)[a]				
0.31	0.934	0.584	0.58	0.42
1.6	0.989	0.683	0.505	0.495
3.1	0.785	0.541	0.505	0.495
pH[b]				
6.5	0.785	0.541	0.505	0.495
9.3	0.874	0.451	0.44	0.56
11.3	1	0.499	0.456	0.544
13.4	1.02	0.569	0.493	0.507
temp (K)[c]				
25	0.785	0.541	0.505	0.495
40	1.01	0.665	0.492	0.508
45	0.971	0.598	0.497	0.503
50	1.31	0.867	0.502	0.498
60	1.51	0.97	0.501	0.499

[a] pH 6.5, 25 °C. [b] 3 wt %, 25 °C. [c] 3 wt %, pH 6.5.

Concentration, pH, and Temperature Effects. To better define the nature of the relationship between the slow and the fast diffusing populations, the concentration, pH, and temperature dependence were characterized for the case of the C_8E_{35} HASE AP. Details are provided in Table 3.

For the HASE APs, NMR signals of adequate intensity can only be obtained at concentrations greater than approximately 0.1 wt %. Remarkably, there is little effect of concentration, at least in this range, on either the diffusion coefficients or the fractional populations

of slow and fast diffusing components. This indicates that the polymer associations leading to the observed diffusion behavior persist at concentrations lower than can be accessed via NMR. There is evidence to support this notion. Specifically, the light scattering results of Dai et al.[20] on the $C_{16}E_{35}$ HASE AP indicate that the diffusion coefficients of the fast and slow diffusing populations are nearly constant over this concentration range and that intermolecular associated structures persist even at concentrations as low as 0.005 wt %. Moreover, fluorescence studies indicate that hydrophobic domains form in the case of $C_{20}E_{35}$ at concentrations as low as 0.01 wt %.[17a]

For the C_8E_{35} HASE AP at 2 wt %, pH has no major effect on the diffusion coefficients of the fast or slow diffusing populations or the fractional distribution between the two. At pH greater than 5.7 polymer dissolution occurs as the polymer's acidic groups become ionized, and above pH 9.0 the methacrylic acid groups are completely dissociated.[17a] Evidently, therefore, once the polymer backbone is sufficiently charged that dissolution is achieved, and network formation is accomplished, the hydrophobic associations that dictate the corresponding diffusion properties are little influenced by further charging of the polymer. Indeed, fluorescence measurements of the pyrene excimer/monomer emission ratio in HASE AP $C_{20}E_{35}$ solutions, a parameter indicative of the presence of hydrophobic domains, show little further change above pH 7.0.[17a] Likewise, rheology studies of various HASE AP show that the zero shear viscosity increases up until pH 7.0 and thereafter more-or-less plateaus.[16d]

For the case of the C_8E_{35} HASE AP at 2 wt %, the diffusion coefficient of both the slow and fast diffusing populations increases with increasing temperature, and both follow an Arrhenius-type behavior, exhibiting activation energies of 15.6 kJ mol^{-1} for the fast diffusing population and 13.9 kJ mol^{-1} for the slow diffusing population. The proportion of the two populations, however, did not change as a function of temperature. These activation energies are lower than those calculated from the temperature dependence of the zero shear viscosity for the $C_{20}E_{35}$ HASE AP[16e] where values on the order of 49.5 kJ mol^{-1} were reported for 0.5 wt % solutions. These authors equate the activation process to dissociation of the hydrophobes from hydrophobic junctions. Consequently, a lower activation energy is to be expected for the C8 hydrophobe examined by PGSE NMR versus the C20 hydrophobe examined by rheology.

Origin of the Diffusional Heterogeneity of HASE AP. The diffusion behavior of the HASE AP solutions reported here reflects the major trends in their rheological properties.[15,16] Specifically, HASE AP structural variables which influence zero shear viscosity enhancement, such as the PEO spacer arm length[16h] or the hydrophobe chain length,[16c] are mirrored qualitatively in the overall HASE AP diffusion behavior. Likewise, environmental variables, such as concentration, pH, and temperature, produce effects on HASE AP diffusion which mirror their established rheological effects.[16d,e] Rheology does not reveal microscopic details of the network morphology. Static and dynamic light scattering, however, do and indicate a bimodal size distribution of diffusing particles in solutions of HASE AP,[20] a situation confirmed here via PGSE NMR. Light scattering, nevertheless, does not reveal whether there

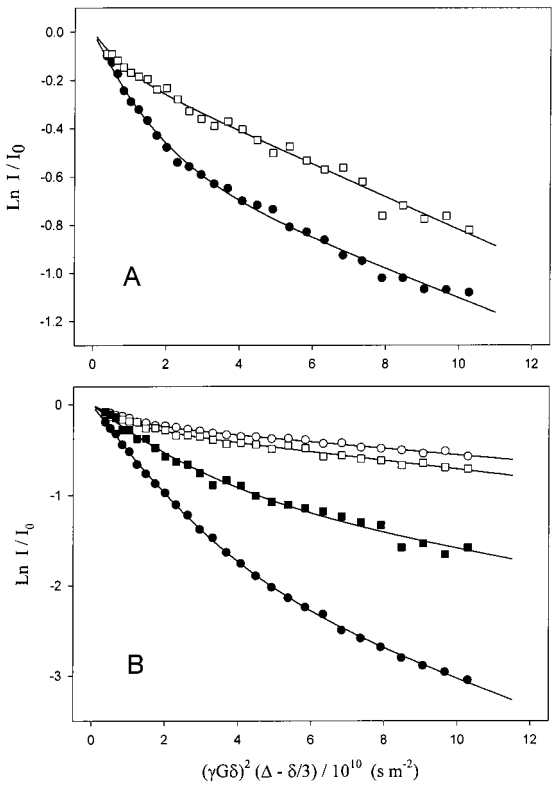

Figure 7. (A) PGSE NMR intensity decays for unfractionated C_4E_{35} HASE AP in DMSO-d_6. Circles: PEO resonance decay ($X_s = 0.604$, $D_s = 6.0 \times 10^{-12}$ m^2 s^{-1}, $X_f = 0.396$, $D_f = 7.2 \times 10^{-11}$ m^2 s^{-1}). Squares: EA-methyl resonance decay (($X_s = 0.870$, $D_s = 6.8 \times 10^{-12}$ m^2 s^{-1}, $X_f = 0.130$, $D_f = 1.2 \times 10^{-10}$ m^2 s^{-1}). Solid lines are the fits to the data using eq 4 and the parameters listed in parentheses. (B) Fractionated HASE AP. Open symbols: THF−HCl-insoluble fraction. Circles: PEO resonance decay ($X_s = 0.821$, $D_s = 3.6 \times 10^{-12}$ m^2 s^{-1}, $X_f = 0.179$, $D_f = 1.1 \times 10^{-10}$ m^2 s^{-1}). Squares: EA-methyl resonance decay ($X_s = 0.792$, $D_s = 4.8 \times 10^{-12}$ m^2 s^{-1}, $X_f = 0.208$, $D_f = 1.1 \times 10^{-10}$ m^2 s^{-1}). Closed symbols: THF−HCl-soluble fraction. Circles: PEO resonance decay ($X_s = 0.204$, $D_s = 1.5 \times 10^{-11}$ m^2 s^{-1}, $X_f = 0.796$, $D_f = 6.4 \times 10^{-11}$ m^2 s^{-1}). Squares: EA-methyl resonance decay ($X_s = 0.412$, $D_s = 7.3 \times 10^{-12}$ m^2 s^{-1}, $X_f = 0.588$, $D_f = 4.7 \times 10^{-11}$ m^2 s^{-1}). Solid lines are the fits to the data using eq 4 and the parameters listed in parentheses.

exists a chemical basis for the observed diffusional heterogeneity. NMR in general, and PGSE NMR in particular, is capable of chemical differentiation and can be used to inquire whether the observed diffusional heterogeneity has a chemical basis.

Figure 7A shows the PGSE NMR intensity decays for the C_4E_{35} HASE AP in DMSO. In DMSO hydrophobic associations are reduced, if not eliminated entirely, relative to aqueous solutions. In addition, the methacrylic acid residues have been protonated, so that chains are not extended by electrostatic repulsion between segments. Overall, viscosity is reduced and NMR line widths for the HASE AP are narrower. The advantage from an NMR perspective is that it is now possible to observe the behavior of different chemical groups in the PGSE NMR experiment. In particular, it is possible to differentiate the PEO spacer arm and the EA methyl resonances, thereby permitting independent monitoring of the macromonomer and the polymer backbone. Figure 7A shows that the PEO spacer arm exhibits a bimodal intensity decay in DMSO similar to that observed in water, as may be ascertained by comparison with Figure 3B. The particulars of the slow

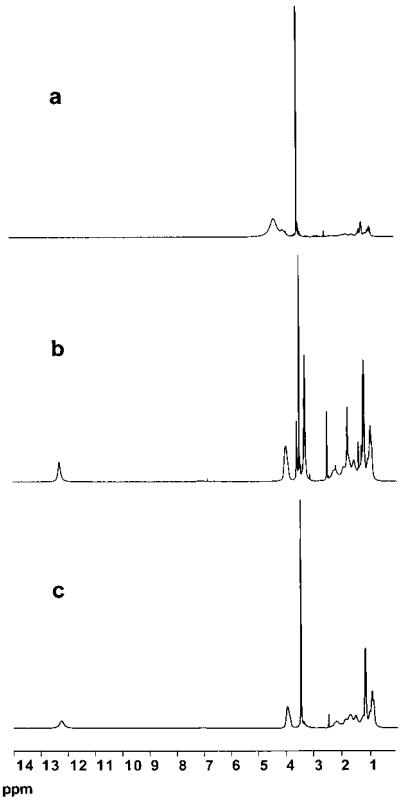

Figure 8. ^{1}H NMR spectra of various C_4E_{35} HASE AP fractions in DMSO-d_6. The unfractionated HASE AP (spectrum c) was precipitated from THF−HCl as described in the text, yielding a precipitate (54 wt %, spectrum b) and a soluble fraction (46 wt %, spectrum a). Their monomer compositions, as obtained from the ^{1}H NMR spectra, are recorded in Table 3.

and fast diffusion coefficients and relative populations are obtained by applying eq 4. However, when the behavior of the EA methyl group is monitored, a more-or-less monomodal intensity decay is obtained. The latter may be fit using eq 3 with $\beta = 0.80$. This indicates that a continuous distribution of diffusion coefficients about a single average value is sufficient to explain the diffusional behavior of the polymer backbone itself. Remarkably, the slower diffusing population from the PEO spacer arm perspective displays a diffusion coefficient nearly identical to the effective diffusion coefficient from the EA methyl group perspective. Similar behavior is exhibited by the two other HASE APs investigated in this fashion, C_8E_{35} and $C_{16}E_{35}$. We conclude that a portion of the macromonomer is able to diffuse independent of the majority of the polymer chains.

Such an effect would arise if the macromonomer was heterogeneously distributed with respect to the polymer chain. To test this possibility, HASE AP C_4E_{35} was dissolved in THF and fractionated by the addition of aqueous HCl which resulted in precipitation of roughly half of the initial material. The ^{1}H NMR spectra of the THF−HCl-soluble and -insoluble materials dissolved in DMSO are shown in Figure 8. Spectrum C in the figure is from the original mixture and is that used to obtain the global compositional data listed in Table 2. Spectrum B is from the THF−HCl-insoluble fraction and clearly shows a depleted macromonomer content relative to the global average. Spectrum A is from the THF−HCl-soluble fraction and indicates a depletion in MA groups and an enrichment with respect to macromonomer content relative to the global average. The details are provided in Table 4.

Table 4. Composition of HASE APs Fractions from ^{1}H NMR

resonance[a]	no. of protons (nominal)	intensity absolute[b]	intensity normalized[c]	comp (mol %)
	C_4E_{35} THF−HCl Soluble			
MA	1	1000	1000	44.6
EA	2	2443	1221	54.5
MM	140	3002	21	0.9
	C_4E_{35} THF−HCl Insoluble			
MA	1	1000	1000	50.1
EM	2	1971	985	49.4
MM	140	1277	9	0.5
	$C_{16}E_{35}$ THF−HCl Soluble			
MA	1	1000	1000	36.4
EA	2	3440	1720	62.6
MM	140	3745	27	1
	$C_{16}E_{35}$ THF−HCl Insoluble			
MA	1	1000	1000	51.7
EA	2	1851	925	47.8
MM	140	1400	10	0.5

[a] MA refers to resonance "e" assigned to the MA carboxyl proton, EA refers to resonance "b" assigned to the EA ethyl ester methylene protons, and MM refers to resonance "f" assigned to the MM ethylene oxide protons. [b] Intensity of MA resonance is normalized to 1000 in each case. [c] Intensities are normalized with respect to the nominal number of protons giving rise to that resonance.

The macromonomer compositions are calculated by assuming that all PEO spacer arms equal 35 EO units in length, an issue the ^{1}H NMR data do not address. Nor do the ^{1}H NMR data address the issue of HASE AP molecular weight polydispersity, although studies indicate that any such polydispersity is not sufficient to explain the bimodal particle size distribution observed by static and dynamic light scattering.[20b] Evidence does suggest that the EA and MA units are not randomly distributed along the polymer chain but rather that the EA units are arranged in blocks.[20b] The compositions listed in Table 4 indicate further that the distribution of MA and macromonomer between chains is inhomogeneous and, to some degree, inversely proportional.

To test how these chemically distinct HASE AP fractions differ with respect to their diffusion properties, the PGSE NMR diffusion coefficient measurement was performed on the two fractions dissolved in DMSO. To reiterate, DMSO permits the PEO and EA methyl resonances to be resolved, therefore allowing one to separately characterize diffusion of the macromonomer versus polymer chain. The results shown in Figure 7B demonstrate that, for the THF−HCl-insoluble fraction, the PEO and EA methyl resonances produce virtually identical diffusion coefficients. This indicates that within this fraction of the HASE AP the macromonomer is homogeneously distributed among the polymer chains. Furthermore, the distribution of diffusion coefficients is monomodal and rather narrow, and the magnitude of the effective diffusion coefficient matches that of the slow diffusing population in aqueous or DMSO solutions of the unfractionated HASE AP.

As for the THF−HCl-soluble fraction, Figure 7B shows that the PEO and EA methyl resonances yield very different and rather polydisperse diffusion coefficients. Both eqs 4 and 5 fit the data equally well, so it is not possible to differentiate continuous from discontinuous distributions. Regardless, it is clear that considerable chemical heterogeneity must remain within

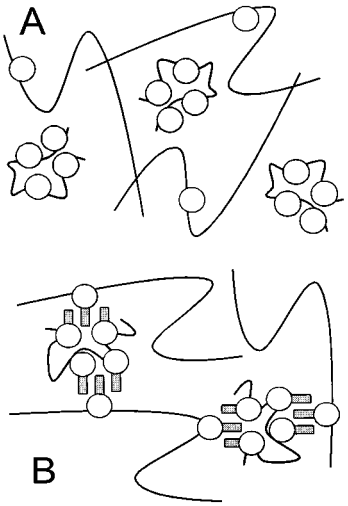

Figure 9. Schematic of HASE AP network microstructure. The polymer backbone is represented as having an extended, relatively rigid conformation due to its polyelectrolyte properties. The PEO spacer arm separating the hydrophobe from the polymer backbone is represented as having a spherical, random coil, relatively flexible conformation. The hydrophobe itself is represented as a rectangular "sticker" group. In panel A, the hydrophobes are either absent or so short that they contribute a negligible tendency to associate. Consequently, the population of polymers with a high macromonomer content has a conformation dominated by its PEO side chains, while the population with a low macromonomer content has a conformation dominated by its polyelectrolyte backbone. Limited association, either intra- or intermolecular, means that the two populations do not couple. In panel B, the hydrophobes are sufficiently long that the tendency to associate is strong. Consequently, the population with a high macromonomer content experiences both intra- and intermolecular hydrophobic associations, while the population with a low macromonomer content undergoes only intermolecular association. Network formation results when the high macromonomer content chains act to bridge between low macromonomer content chains.

this fraction, since the PEO and EA methyl diffusion behavior is so different, and that further fractionation would be possible. The magnitude of the effective diffusion coefficient from the PEO spacer arm resonance of the THF−HCl-insoluble fraction is virtually identical to that of the fast diffusing component in aqueous or DMSO solutions of the unfractionated HASE AP.

Microstructure of HASE AP Networks. These PGSE NMR measurements provide a new perspective on the architecture of HASE AP networks, augmenting the picture obtained from rheology[16] and other[17−20] techniques. The novel insight provided by NMR is that two (or more) distinct diffusing species coexist and that these species differ markedly with respect to their macromonomer and MA content. How this might influence network properties, within the context of the current understanding of HASE APs, is presented schematically in Figure 9.

Thickening in HASE AP solutions is the result of a combination of hydrophobic association and polymer entanglement. At high pH the MA units of the HASE AP backbone are ionized, which produces chain expansion and thickening through conventional hydrodynamic volume and chain entanglement effects. The hydrophobic groups of the HASE AP assemble into association sites through mutual attraction, which leads to thickening through the formation of a transient network. The PEO spacer arm separating the hydrophobe from the polymer backbone permits freer association of hydrophobes, thereby encouraging network formation. Longer hydrophobe chains have a greater tendency to associate, which likewise encourages network formation. The longer the hydrophobe, the greater the number of, and the greater the strength of, individual hydrophobic junctions.

The preeminent role of the hydrophobe is evident from Figure 3, where, at constant PEO spacer arm length, diffusion is extremely sensitive to the length of the hydrophobe. At constant hydrophobe length, in contrast, the effect of the PEO spacer arm length is secondary. Therefore, in discussing the effects of chemical heterogeneity in HASE AP on the tendency to associate, our attention will focus on the hydrophobe. The PEO spacer arm is highly flexible and approximated as a random coil, depicted in Figure 9 as a spherical "blob". One recognizes that in hydrophobic junctions with large aggregation numbers the average PEO configuration may become distorted.

In the schematic, the notion of chemical heterogeneity is simplified to two situations. In the first, there are very few macromonomers per chain and a high MA content, so that the charged groups on the polymer backbone dictate the behavior, producing an extended chain conformation. In the second, there are a multitude of macromonomers per chain and relatively few MA residues, so that the PEO spacer arm and/or the hydrophobe dictate the behavior. If the hydrophobe is short, as depicted in Figure 9 (panel A), then the tendency to associate is weak. Intramolecular associations are probable, given a high local hydrophobe concentration. This, in combination with a lower linear charge density, produces a compact structure relative to the situation with fewer macromonomers and more MA units per chain. It is likely that these structures consist of single chains. Intermolecular associations between the two types of chains are few and weak. If the hydrophobe is long, as depicted in Figure 9 (panel B), then the tendency to associate is strong. Intramolecular associations and a lower linear charge density again produce a compact structure. However, intermolecular associations between the two types of chains are also likely, driven by the hydrophobes tendency to associate.

The scenario depicted in Figure 9 is consistent, not only with the PGSE NMR data reported here but also with the rheology data[16] and static and dynamic light scattering reports[20] on HASE APs. Both light scattering and PGSE NMR studies indicate that HASE AP solutions contain two components, a fast diffusing population and a slow diffusing population. The two techniques produce comparable numbers for the diffusion coefficients and relative populations of the two components. The NMR results demonstrate further, however, that the presence of these two populations originates in the chemical heterogeneity of macromonomer and MA distribution within the HASE AP population.

HASE APs are synthesized by emulsion polymerization, i.e., a free radical initiated, multiphase process.[15b] It is not surprising therefore that heterogeneity of composition results, since the composition will depend on the different monomer reactivity ratios and the water solubility of the different monomers, as well as the method of feed of monomers during the emulsion polymerization process. A detailed study of the monomer reactivity ratios would appear to be the next step to advance the science.

References and Notes

(1) (a) *Water Soluble Polymers*; Glass, J. E., Ed.; ACS Advances in Chemistry Series 213; American Chemical Society: Washington, DC, 1986. (b) *Polymers in Aqueous Media*; Glass, J. E., Ed.; ACS Advances in Chemistry Series 213; American Chemical Society: Washington, DC, 1989. (c) *Hydrophobic Polymers: Performance with Environmental Acceptance*; Glass, J. E., Ed.; ACS Advances in Chemistry Series 248; American Chemical Society: Washington, DC, 1996. (d) *Polymers as Rheology Modifiers*; Schulz, D. N., Glass, J. E., Eds.; ACS Symposium Series 462; American Chemical Society: Washington, DC, 1991.

(2) (a) Jenkins, R. D. Ph.D. Thesis, Lehigh University, Bethlehem, PA. (b) Jenkins, R. D.; Silebi, C. A.; El-Aasser, M. S. *Polym. Mater. Sci. Eng.* **1989**, *61*, 629. (c) Jenkins, R. D.; Silebi, C. A.; El-Aasser, M. S. In *Advances in Emulsion Polymerization and Latex Technology; 21st Annual Short Course*; El-Aasser, M. S., Ed.; Lehigh University: Bethlehem, PA, June 1990; Chapter 17.

(3) (a) Maechling-Strasser, C.; Francois, J.; Clouet, F.; Tripette, C. *Polymer* **1992**, *33*, 627. (b) Maechling-Strasser, C.; Clouet, F.; Francois, J. *Polymer* **1992**, *33*, 1021. (c) Persson, K.; Abramsen, S.; Stilbs, P.; Hansen, F. K.; Walderhaug, H. *Colloid Polym. Sci.* **1992**, *270*, 465. (d) Fonnum, G.; Bakke, J.; Hansen, F. K. *Colloid Polym. Sci.* **1993**, *271*, 380.

(4) (a) Annable, T.; Buscall, R.; Ettalaie, R.; Wittlestone, D. *J. Rheol.* **1993**, *37*, 695. (b) Annable, R.; Buscal, R.; Ettelaie, R. *Colloids Surf. A* **1996**, *112*, 97. (c) Annable, T.; Buscall, R.; Shepherd, P.; Whittlestone, D. *Langmuir* **1994**, *10*, 1060.

(5) (a) Wang, Y.; Winnik, M. A. *Langmuir* **1990**, *6*, 1437. (b) Yekta, A.; Duhamel, J.; Brochard, P.; Adiwidjaja, H.; Winnik, M. A. *Macromolecules* **1993**, *26*, 1829. (c) Yekta, A.; Duhamel, J.; Adiwidjaja, H.; Brochard, P.; Winnik, M. A. *Langmuir* **1993**, *9*, 881. (d) Yekta, A.; Xu, B.; Duhamel, J.; Adiwidjaja, H.; Winnik, M. A. *Macromolecules* **1995**, *28*, 956.

(6) (a) Rao, B. H.; Uemura, Y.; Dyke, L.; Macdonald, P. M. *Macromolecules* **1995**, *28*, 531. (b) Uemura, Y.; Macdonald, P. M. *Macromolecules* **1996**, *29*, 63. (c) Zhang, K.; Xu, B.; Winnik, M. A.; Macdonald, P. M. *J. Phys. Chem.* **1996**, *100*, 9834.

(7) (a) Xu, B.; Zhang, K.; Macdonald, P. M.; Winnik, M. A.; Jenkins, R.; Bassett, D.; Wolf, D.; Nuyken, O. *Langmuir* **1997**, *13*, 6896. (b) Xu, B.; Yekta, A.; Winnik, M. A.; Sadeghy-Dalivand, K. James, D. F.; Jenkins, R.; Bassett, D. *Langmuir* **1997**, *13*, 6903. (c) Xu, B.; Yekta, A.; Masoumi, Z.; Kanagalingam, S.; Winnik, M. A.; Zhang, K.; Macdonald, P. M. *Langmuir* **1997**, *13*, 2447.

(8) (a) Landoll, L. M. *J. Polym. Sci., Polym. Chem. Ed.* **1982**, *20*, 443. (b) Sau, A. C.; Landoll, L. M. In *Polymers in Aqueous Media: Performance Through Association*; Glass, J. E., Ed.; ACS Advances in Chemistry Series 223; American Chemical Society: Washington, DC, 1989; p 343.

(9) Gelman, R. A.; Barth, H. G. In *Water Soluble Polymers: Beauty with Performance*; Glass, J. E., Ed.; ACS Advances in Chemistry Series 213; American Chemical Society: Washington, DC, 1986; p 101.

(10) (a) Aubry, T.; Moan, M. *J. Rheol.* **1994**, *38*, 1681. (b) Aubry, T.; Moan, M. *J. Rheol.* **1996**, *40*, 441.

(11) (a) Godwin, J. W.; Highes, R. W.; Lam, C. K.; Miles, J. A.; Warren, B. C. H. In *Polymers in Aqueous Media: Performance through Association*; Glass, J. E., Ed.; ACS Advances in Chemistry Series 223; American Chemical Society: Washington, DC, 1989; p 365. (b) Young, T. S.; Fu, E. *Tappi J.* **1991**, *74*, 197. (c) Tanaka, R.; Meadows, J.; Williams, P. A.; Philips, G. O. *Carbohydr. Polym.* **1990**, *12*, 443. (d) Tanaka, R.; Meadows, J.; Williams, P. A.; Philips, G. O. *Macromolecules* **1992**, *25*, 1304. (e) Tanaka, R.; Williams, P. A.; Meadows, J.; Philips, G. O. *Colloids Surf.* **1992**, *66*, 63. (f) Sividasan, K.; Somasundaran, P. *Colloids Surf.* **1990**, *49*, 229.

(12) (a) Kastner, U.; Hoffmann, H.; Donges, R.; Ehrler, R. *Colloids Surf. A* **1994**, *82*, 279. (b) Kastner, U.; Hoffmann, H.; Donges, R.; Ehrler, R. *Colloids Surf. A* **1996**, *112*, 209.

(13) (a) Thuresson, K.; Nilsson, S.; Lindman, B. *Langmuir* **1996**, *12*, 530. (b) Thuresson, K.; Nyström, B.; Wang, G.; Lindman, B. *Langmuir* **1995**, *11*, 3730. (c) Thuresson, K.; Söderman, O.; Hansson, P.; Wang, G. *J. Phys. Chem.* **1996**, *100*, 4909.

(14) Varelas, C. G.; Dualeh, A. J.; Steiner, C. A. In *Macromolecular Complexes in Chemistry and Biology;* Dubin, P., Bock, J., Davis, R., Schulz, D. N., Theis, C., Eds.; Springer-Verlag: Berlin, 1994; p 63.

(15) (a) Shay, G. D. In *Polymers in Aqueous Media: Performance Through Association*; Glass, J. E.; Ed.; ACS Advances In Chemistry Series 223; American Chemical Society: Washington, DC, 1989; p 457. (b) Jenkins, R. D.; DeLong, L. M.; Bassett, D. R. In *Hydrophilic Polymers: Performance with Environmental Acceptability*; Glass, J. E.; Ed.; ACS Advances in Chemistry Series 248; American Chemical Society: Washington, DC, 1996; p 425. (c) Wong, S. Y.; Tam, K. C.; Jenkins, R. D. *Proc. 2nd National Undergraduate Research Programme Congress* **1997**, *3*, 1652.

(16) (a) English, R. J.; Gulati, H. S.; Jenkins, R. D.; Khan, S. A. *J. Rheol.* **1997**, *41*, 427. (b) Tirtaatmadja, V.; Tam, K. C.; Jenkins, R. D. *Macromolecules* **1997**, *30*, 1426. (c) Tirtaatmadja, V.; Tam, K. C.; Jenkins, R. D. *Macromolecules* **1997**, *30*, 3271. (d) Tam, K. C.; Farmer, M. L.; Jenkins, R. D.; Bassett, D. R. *J. Polym Sci., Part B: Polym. Phys.* **1998**, *36*, 2275. (e) Tirtaatmadja, V.; Tam, K. C.; Jenkins, R. D. *Langmuir* **1999**, *15*, 7537. (f) Tam, K. C.; Guo, L.; Jenkins, R. D.; Bassett, D. R. *Polymer* **1999**, *40*, 6369. (g) Seng, W. P.; Tam, W. C.; Jenkins, R. D. *Colloids Surf. A* **1999**, *154*, 365. (h) Seng, W. P. M. Eng. Thesis, Nanyang Technological University, Singapore, 1999.

(17) (a) Kumacheva, E.; Rharbi, Y.; Winnik, M. A.; Guo, L.; Tam, K. C.; Jenkins, R. D. *Langmuir* **1997**, *13*, 182. (c) Horiuchi, K.; Rharbi, Y.; Spiro, J. G.; Yekta, A.; Winnik, M. A.; Jenkins, R. D.; Bassett, D. R. *Langmuir* **1999**, *15*, 1644.

(18) (a) Guo, L.; Tam, K. C.; Jenkins, R. D. *Macromol. Chem. Phys.* **1998**, *199*, 1175. (b) Ng, W. K.; Tam, K. C.; Jenkins, R. D. *Eur. Polym. J.* **1999**, *35*, 1245.

(19) (a) Seng, W. P.; Tam, K. C.; Jenkins, R. D.; Bassett, D. R. *Langmuir* **2000**, *16*, 2151. (b) Seng, W. P.; Tam, K. C.; Jenkins, R. D.; Bassett, D. R. *Macromolecules* **2000**, *33*, 1727.

(20) (a) Seng, W. P.; Tam, K. C.; Jenkins, R. D. *Macromolecules* **2000**, *33*, 404. (b) Islam, M. F.; Jenkins, R. D.; Bassett, D. R.; Lau, W.; Ou-Yang, H. D. *Macromolecules* **2000**, *33*, 2480.

(21) (a) Stejskal, E. O.; Tanner, J. E. *J. Chem. Phys.* **1965**, *45*, 288. (b) Tanner, J. E.; Stejskal, E. O. *J. Chem. Phys.* **1968**, *49*, 1768.

(22) Mills, R. *J. Phys. Chem.* **1973**, *77*, 685.

(23) von Meerwall, E. D. *J. Magn. Reson.* **1982**, *50*, 409.

(24) Walderhaug, H.; Hansen, F.; Abramsen, S.; Persson, K.; Stilbs, P. *J. Phys. Chem.* **1993**, *97*, 8336.

(25) Nyström, B.; Walderhaug, H.; Hansen, F. K. *J. Phys. Chem.* **1993**, *97*, 7743.

(26) Uemura, Y.; McNulty, J.; Macdonald, P. M. *Macromolecules* **1995**, *28*, 4150.

(27) (a) Morris, K. F.; Johnson, C. S., Jr. *J. Am. Chem. Soc.* **1992**, *114*, 3139. (b) Morris, K. F.; Johnson, C. S., Jr. *J. Am. Chem. Soc.* **1993**, *115*, 4291.

MA0013004